

# Brain morphometry driven by DTI data in Moebius Syndrome and Hereditary Congenital Facial Paresis

Neda Sadeghi<sup>1</sup>, Irimi Manoli<sup>2</sup>, Elizabeth Hutchinson<sup>3</sup>, Carol Van Ryzin<sup>2</sup>, Cibu Thomas<sup>4</sup>, M. Okan Irfanoglu<sup>3</sup>, Amritha Nayak<sup>3</sup>, Chia-Ying Liu<sup>5</sup>, Francis S. Collins<sup>2</sup>, Ethylin Wang Jabs<sup>6</sup>, Elizabeth C. Engle<sup>7,8</sup>, Carlo Pierpaoli<sup>3</sup>, and the Moebius Collaborative Research Group

<sup>1</sup>Section on Quantitative Imaging and Tissue Sciences, Eunice Kennedy Shriver National Institute of Child Health and Human Development, National Institutes of Health, Bethesda, MD, USA, <sup>2</sup>Medical Genomics and Metabolic Genetics Branch, National Human Genome Research Institute, National Institutes of Health, Bethesda, MD, USA, <sup>3</sup>Quantitative Medical Imaging Section, National Institute of Biomedical Imaging and Bioengineering, National Institutes of Health, Bethesda, MD, USA, <sup>4</sup>National Institute of Mental Health, Bethesda, MD, USA, <sup>5</sup>Radiology and Imaging Sciences, National Institutes of Health, Bethesda, MD, USA, <sup>6</sup>Department of Genetics and Genomic Sciences, Icahn School of Medicine at Mount Sinai, New York, NY, USA, <sup>7</sup>Departments of Neurology and Ophthalmology, Boston Children's Hospital and Harvard Medical School, Boston, Massachusetts, <sup>8</sup>Howard Hughes Medical Institute, Chevy Chase, MD, United States

## Introduction :

Moebius syndrome (MBS) is a rare birth defect condition characterized by paralysis or weakness of facial muscles and impairment of ocular abduction. Although these features are the minimum criteria for diagnosis [1,2,3], reported morphological abnormalities in brain imaging studies of MBS patients have varied. MBS can be differentiated from hereditary congenital facial paresis (HCFP), where extraocular movements are normal. We performed a brain imaging study of MBS and HCFP patients and controls to investigate morphological differences between these groups. We used a newly developed tensor based morphometry (TBM) approach in which deformation fields are extracted from diffusion tensor imaging data [4] rather than T1-weighted (T1W) images as typically done [5]. This approach, which we call D-TBM for diffusion driven TBM, enables a better identification of morphological changes of individual white matter pathways compared to T1W driven TBM [6].

## Methods:

Patients diagnosed with MBS (n=9, 8 females, 1 male, mean age=40 years, range 21-64) and HCFP (n=5, 2 females, 3 males, mean=37 years, range 12-57) along with 15 controls (10 females, 5 males, mean age= 34 years, range 14-55) were included in this study. Five of the MBS patients had limb malformations in addition to facial palsy and impairment of ocular abduction. All participants were scanned on a Philips 3T system with 8-channel head coil. The DTI data were acquired with a single-shot spin-echo echo-planar imaging sequence (TR: 10.5 s, TE: 85 ms, slices=90, voxel size=2x2x2 mm). Acquisition consisted of seven low b-values (b=0 and 50 s/mm<sup>2</sup>), and 39 volumes with maximum b-value of 1100 s/mm<sup>2</sup>. The sequence was repeated four times with phase encoding directions AP, PA, LR, RL. Fat suppressed T2 weighted images were also acquired at 1 x 1 x 2 mm. DWIs were corrected for motion, eddy-

currents, and geometrical distortions [6], subsequently the diffusion tensor (DT) was computed using the nonlinear tensor estimation using TORTOISE package<sup>7</sup>.

For TBM analysis, the images of all subjects in the study needed to be aligned together. Control subjects' DTs were used to create a study-specific control template using DR-TAMAS diffeomorphic tensor-based registration method [9]. Subsequently, all subjects' DTs were registered to the control template. Log of determinant of the Jacobian of transformations that map each individual to the control template was then calculated (LogJ maps). To assess LogJ differences between patients and controls we used the FSL randomise software with threshold-free cluster enhancement [10] corrected for multiple comparisons using a family-wise error rate of  $p < 0.05$ .

### **Results:**

We present the results of voxelwise statistical analysis of LogJ maps in Figure 1. One area of particular interest in comparison of the MBS patients to the control group is the brainstem. The statistical results of D-TBM revealed volumetric reduction in the brainstem (posterior pons), indicating atrophy or hypoplasia of the brainstem at this level. The pontine tegmentum contains the nuclei of cranial nerves VI, VII, and the medial longitudinal fasciculus. Similar abnormalities were also observed for the subset of MBS patients with limb defects. However, HCFP did not show hypoplasia in this region. There was no additional significant volume increase or decrease throughout the brain besides the brainstem.

### **Conclusions:**

Our D-TBM analysis reveals that there is a significant decrease in volume of the pontine tegmentum region of the brainstem in MBS, irrespective of extracranial manifestations. Interestingly, HCFP patients did not show any significant volume decrease compared to the control group. This provides supporting evidence that hypoplasia of brainstem at this level may serve as a biomarker of MBS, and that MBS and HCFP are two distinct clinical entities.

Support for this work included funding from U01 HD079068-01 grant, HJF Awards: 30613610.0160855 and W81XWH-13-2-0019.

### **References**

1. Verzijl, H.T.F.M. et al. (2003), 'Möbius syndrome redefined A syndrome of rhombencephalic maldevelopment', *Neurology*, vol. 61, no. 3, pp. 327-333
2. Webb, B.D. et al. (2012), 'HOXB1 founder mutation in humans recapitulates the phenotype of Hoxb1<sup>-/-</sup> mice', *Am. J. Hum. Genet.* vol. 91, pp. 171-179
3. MacKinnon, S. et al. (2014). 'Diagnostic distinctions and genetic analysis of patients diagnosed with Moebius syndrome', *Ophthalmology*, vol. 121, no. 7, pp. 1461-1468
4. Basser, P.J. et al. (1994). 'Estimation of the effective self-diffusion tensor from the NMR spin echo', *J Magn Reson B*, vol. 103, no. 3, pp. 247-254
5. Ashburner, J. et al. (1998). 'Identifying global anatomical differences: deformation-based morphometry', *Human brain mapping*, vol. 6, pp. 348-357

6. Sadeghi, N. et al. (2016). 'Deformation analysis of diffusion tensor data: application to Hereditary Spastic Paraplegia', ISMRM 24<sup>th</sup> annual meeting, Singapore.
7. Irfanoglu, M.O. et al. (2015). 'DR-BUDDI (Diffeomorphic Registration for Blip-Up Blip-Down Diffusion Imaging) method for correcting echo planar imaging distortions', NeuroImage, vol. 106, pp. 284-299
8. Pierpaoli, C. et al. (2010), 'TORTOISE: an integrated software package for processing of diffusion MRI data', ISMRM 19th annual meeting, Stockholm, Sweden
9. Irfanoglu, M.O. et al. (2016), 'DR-TAMAS: Diffeomorphic registration for tensor accurate alignment of anatomical structures', NeuroImage, vol. 132, pp. 439-454
10. Smith, S. M. et al. (2009), 'Threshold-free cluster enhancement: addressing problems of smoothing, threshold dependence and localisation in cluster inference', Neuroimage, vol. 44, pp. 83-98

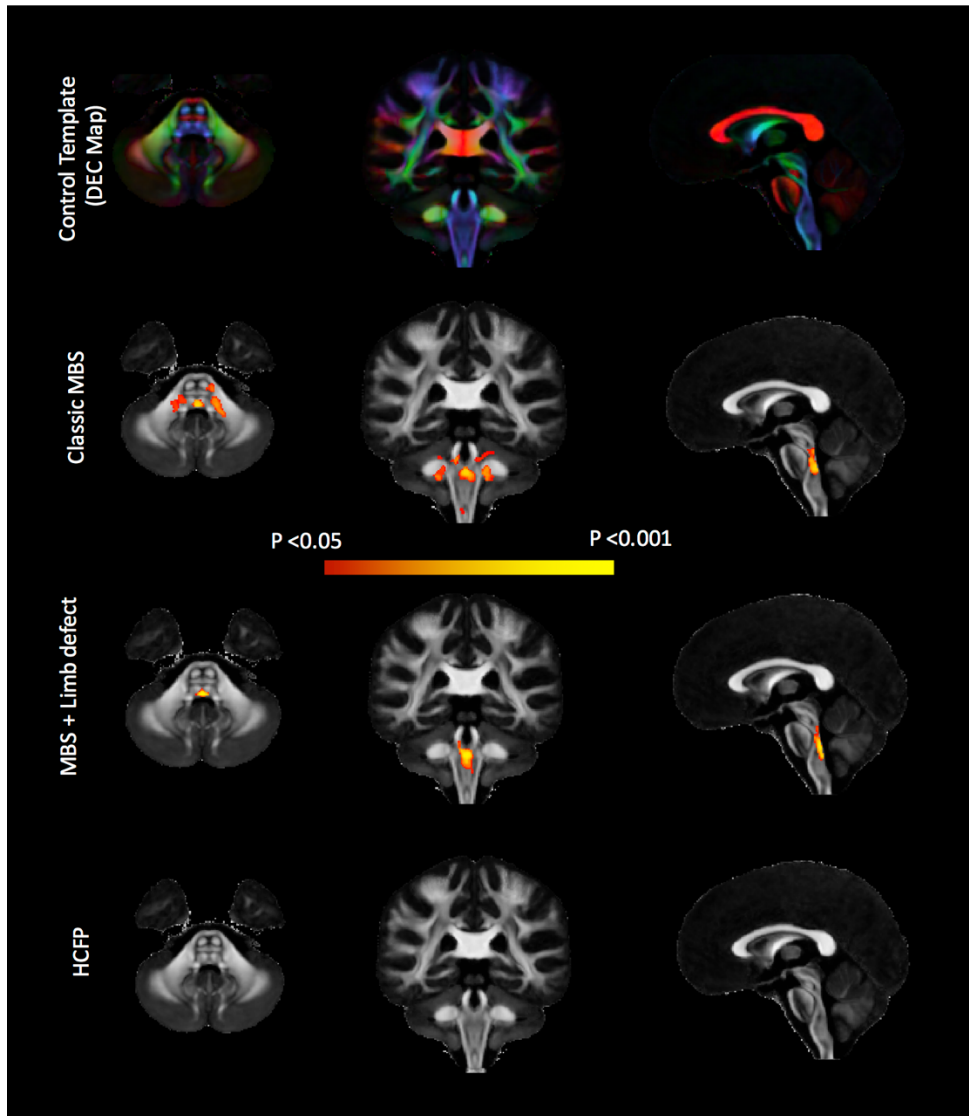


Figure 1. Areas of significant volumetric reduction in patients compared to controls superimposed on FA map of the control template. Top: corresponding directionally encoded color (DEC) map.